British Journal of Earth Sciences Research, 12 (1),42-60,2024

Print ISSN: 2055-0111 (Print)

Online ISSN: 2055-012X (Online)

Website: https://www.eajournals.org/

Publication of the European Centre for Research Training and Development -UK

Application of Post Stack Acoustic Impedance Inversion to Lateral Rock Property Prediction: A Case Study Eti-field Offshore Niger Delta

Ede Tiekuro[1*], Godwin Omokenu Emujakporue[2], Cyril N. Nwankwo[2]

[1]Department of Physics, School of Basic Science, Nigeria Maritime University Okerenkoko, Delta State Nigeria.

[2]Department of Physics, University of Port Harcourt, Port Harcourt, Nigeria.

doi : https://doi.org/10.37745/bjesr.2013/vol12n14260 Published March 08, 2024

Citation: Tiekuro E., Emujakporue G.O., and Nwankwo C.N. (2024) Application of Post Stack Acoustic Impedance Inversion to Lateral Rock Property Prediction: A Case Study Eti-field Offshore Niger Delta, *British Journal of Earth Sciences Research*, 12 (1),42-60

ABSTRACT: *This study presents the result of a Model-based seismic inversion technique which was used to invert an acoustic impedance structure within a reservoir interval by intergrating well logs and 3D post stack seismic data obtained from Eti-field offshore Niger Delta. The purpose was to delineate lateral and vertical alternations in subsurface rock properties which is caused by difference in lithofacies within the reservoir interval. This would help to define hydrocarbon fairways better and constrain the range of hydrocarbon zones for field development. The inversion workflow used in this study includes forward modelling of reflection coefficients from a low frequency impedance model driven from well logs and convolution of the reflection coeffiecients with a source wavelet derived from the seismic data. P-impedance inversion analysis at the control well location gave a near perfect correlation of 0.993686 (correlation coefficient of ≈ 99.4 %) between the original P-impedance log, initial guess P-impedance model log and inverted P-impedance log. The estimated error observed was 5533.1 which corresponds to (0.112308) about 11.23 %. Seismic inversion analysis realized an acoustic impedance striucture with P-impedance values ranging from 7000 to about 50000 ft/s*g/cc and having a general increase with depth trend. Impedance slice extracted from the impedance volume at top of the reservoir predicted lateral variations in P-impedance at well control and away from well control. This information can be invaluable in delineating more prospective reservoir zones in the field and thereby enhancing optimum field development which aids in reservoir management decisions.*

KEYWORDS: Acoustic impedance, Seismic inversion, Model-based, Hamson-Russell strata software (HRS), Lateral property prediction.

INTRODUCTION

According to Sheriff (2002), as cited by Okoli *et al*., (2018), geophysical inversion can be defined as a technique that provides solution to spatial distribution of parameters which could have produced an observed set of measurements. For the seismic case, the observation consists of the physical signature of a subsurface structure i:e the structure's reflected (or scattered) as a wave field due to a seismic source signal. Therefore, it is imperative to select a forward modeling procedure that can adequately define the set of observations. For the acoustic impedance case the defined set of parameters are "layer velocities and layer densities". Therefore, the choice of the actual model is vital and depends on the exploration problem to be resolved.

In quantitative seismic interpretation, effort is made to retrieve rock properties from seismic data using the inversion technique so as to obtain meaningful results for reservoir characterization (Hafez and Castagna, 2016; Parvaneh, 2015). The ability to estimate rock properties from seismic data increases the interpreter's ability to discriminate between different lithofacies and fluid types (Ogagarue 2016; Jason *et al*., 2008; Duffaut *et al*., 2000), resulting in a detailed stratigraphic/reservoir imaging for improved hydrocarbon recovery.

Unlike seismic reflection dataset (which is a boundary-based property) acoustic impedance is a rock property and is the product of rock density and p-wave velocity. Acoustic impedance inversion involves conversion of seismic traces to a reflection coefficient time series, and then into an acoustic impedance trace (Eze et al., 2019; Ogagarue and Alaminiokuma 2016; Parvaneh 2015; Jason *et al*., 2008; Lavergne and William 1977; Lindseth, 1979). These impedance traces will help augment the accuracy of interpretation and correlation with properties measured in well logs.

In this sense, impedance inversion can be considered a sophisticated method of integrating well logs and seismic data for lateral rock property prediction to optimize hydrocarbon production (Eze et al., 2019; Ogagarue and Alaminiokuma 2016; Ahmed and John 2016; Nadin and Kusznir 1995). The model-based inversion strategy converts seismic data to a pseudo-acoustic impedance log at every trace. Acoustic impedance dataset is utilized in producing more accurate and detailed seismic interpretation than can not be obtained from seismic (or seismic attribute) interpretation. This serves as an improvement over conventional seismic interpretation which relies on the seismic data alone to map geological structures suitable for hydrocarbon accumulation (Eze et al., 2019; Ogagarue and Alaminiokuma 2016).

This present study is aimed at applying a model-based inversion technique to invert acoustic impedance dataset from seismic data and interprete results for lateral rock property prediction. The model-based acoustic impedance inversion is actualized based on the generalized linear inversion (GLI) reported by Cooke and Schneider (1983), as cited by Ogagarue and Alaminiokuma (2016); Parvaneh (2015); and Jason *et al*., (2008).
The generalized linear inversion employs the Taylor series expansion;

$$S(M) = S(Mi) + \frac{\partial S(Mi)}{\partial M}\Delta M + \cdots \quad (1)$$

Where;
Mi = initial model
M = real model
ΔM= change in model parameters
S(M) = observed seismic trace
S(Mi) = synthetic seismic from initial model

The strength of the model-based inversion technique is its ability to reduce the difference (ΔS) between the observed seismic trace S(M) and the synthetic seismic S(Mi) obtained from the initial model (Eze et al., 2019). The initial model incorporates low frequency information from local wells (Jason *et al*., 2008).

The objective function is reduced by repetitive modification of the model which gives a reasonable solution if the initial guess model is within the region of global convergence of the objective function (Jason *et al.*, 2008; Hampson and Russell, 1999).
The Hampson-Russell strata theory is a highly evolved method that minimizes the following objective function:

$$\mathbf{e} = (\mathbf{T} - \mathbf{wDL}) \qquad (2)$$

Where **e** is the residual difference (in vector notation) between the seismic trace **T** and the trace resulting from the model data **wDL**, where **w** is the convolutional wavelet matrix for an *n* sample wavelet and L is a vector consisting of the logarithm of impedance for *m* model samples and given as

$$L(i) = \log Z(i) \qquad (3)$$

where Z(i) is the impedance model and **D** is an *m*-1 by *m* derivative matrix where m is the number of layers to be solved for and *m*-1 is the number of reflection coefficients (Ogagarue and Alaminiokuma 2016; Jason *et al*., 2008). The addition of the square of the errors is given by:

$$e^T e = (T - wDL)^T (T - wDL) \qquad (4)$$

Using linear inverse theory (Jason *et al*., 2008; Aster *et al*., 2005), minimizing $\mathbf{e^T e}$ leads to the "normal equation" (with a stabilization factor, a) inserted we have:

$$\left((D^T w^T W D) + aI\right)L = D^T w^T T \qquad (5)$$

However, rather than solving Equation (5) directly for **L**, a solution estimate is found by repetitive refinement of a guess at the correct model until $\mathbf{e^T e}$ is minimized (Jason *et al*., 2008). An initial guess model is seeded in Equation (5) for **L** which includes the low frequency trend from regional wells (Ahmed and John 2016; Jason *et al*., 2008).
Conjugant gradient repetition of **L** then minimizes the error $\mathbf{e^T e}$**.** However, since the solution to Equation (5) is non-unique (an infinite number of models can minimize $\mathbf{e^T e}$**)**, constraints are introduced that restricts the possible solutions (Jason *et al.*, 2008; Hampson and Russell, 1999). These constraints are imposed on the upper and lower bounds for the impedance estimates (Yi Zhang *et al*., 2015; Jason *et al*., 2008). The algorithim enables the user to define the bounds as a percentage of the average impedance of the initial guess model and low frequency trend introduced in the initial guess model, is carried through to the final solution since low frequency data is generally not recorded in the seismic data. Also, high frequencies above the seismic bandwidth are carried through if they are not filtered away from the model prior to the inversion (Jason *et al*., 2008).

Print ISSN: 2055-0111 (Print)
Online ISSN: 2055-012X (Online)
Website: https://www.eajournals.org/
Publication of the European Centre for Research Training and Development -UK

From the above precedings, a good model based inversion algorithm will produce high-quality acoustic impedance volumes from post-stack seismic data. The model was based solely on the calculated impedance at log resolution from a control well which was then extrapolated throughout the survey domian. The low-frequency impedance data missing from the seismic data is derived from well logs (Ogagarue and Alaminiokuma 2016; Ahmed and John, 2016). This paper focuses on acoustic impedance inversion and interpretation of results for lateral property prediction at well control and away from the control wells for well placement optimization. The study area is Eti-field located offshore Niger Delta.

GEOLOGIC SETTING

The study area "Eti-Field" is located within the offshore depobelt of the Niger Delta (Figure 1a). The region is a prolific hydrocarbon province formed during three depositional cycles from middle Cretaceous to Recent.

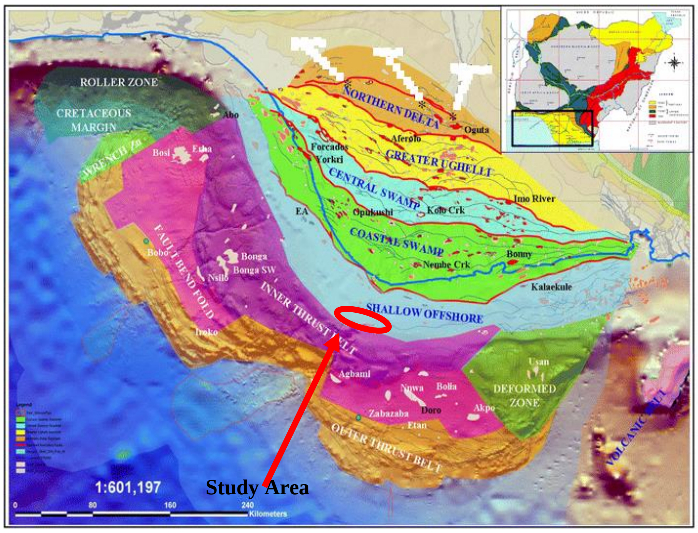

a

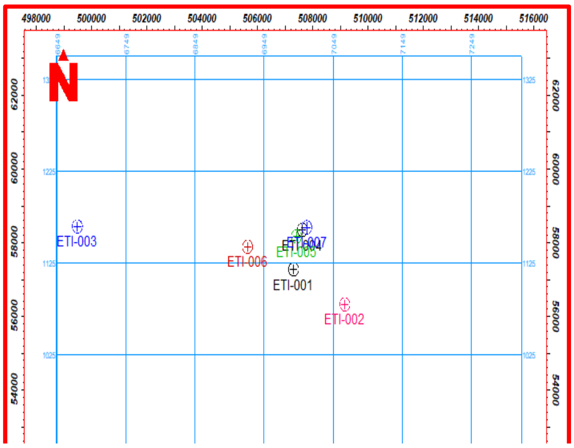

b

Figure 1(a): Map of the study area (Eti-Field) showing location of the study area on Niger Delta map. Figure 1(b): Base map of ETI-Field with seismic grid lines and well positions.

The Niger Delta basin is a prolific hydrocarbon province that evolved in early tertiary times where rapid deposition and subsidence have occurred over time (Doust and Omatsola, 1990). Collectively, the delta is known to have prograded over the subsidizing continental-oceanic lithospheric transition zone, and during the Oligocene spread into oceanic crust of the Gulf of Guinea (Orife and Avbovbo 1982; Short and Stauble 1967). Thickness of sediments in the region averages at 12 km covering a total area of about 140,000 km^2 (Akpabio *et al*., 2014; Agbasi 2013; Alao *et al*., 2013). The early Niger Delta is interpreted as being a river-dominated delta, however the post-Oligocene delta is a typical wave-dominated delta with well-developed shoreface sands, beach ridges, tidal channels, mangrove and freshwater swamps (Orife and Avbovbo 1982; Akpoyovbike 1978; Tamuko 2008). It is one of the world's largest deltas and shows an overall upward transition from marine shales (Akata Formation) through a sand-shale paralic interval (Agbada Formation) to continental sands of the Benin Formation (Michele *et al*., 1999; Akpoyovbike 1978). Depending on relative sea level changes, local subsidence and sediment supply, the delta experiences episodes of regressions and transgressions (Nadin and Kusznir 1995; as cited by Tamuko 2008). The stratigraphic arrangement of the Niger Delta comprises of three wide lithostratigraphic units namely; a continental shallow massive sand sequence – the Benin Formation, a coastal marine sequence of alternating sands and shales – the Agbada Formation and a basal marine shale unit-the Akata Formation (Alao *et al*., 2013; Akpabio *et al.,* 2014; Agbasi 2013). The Akata Formation consists of clays and shales with minor sand alternations (Alao *et al.,* 2013). The sediments were deposited in prodelta environments, with sand percentage collectively less than 30% (Akpabio *et al*., 2014; Alao *et al*., 2013; Agbasi 2013). The Agbada Formation consists of alternating sand and shales representing sediments of the transitional environment comprising the lower delta plain (mangrove swamps, floodplain and marsh) and the coastal barrier and fluvio marine realms (Akpabio *et al.,* 2014; Alao *et al.,* 2013; Agbasi 2013). The sand percentage within the Agbada Formation varies from 30 to 70%, which results from the large number of depositional off lap cycles. A complete cycle generally consists of thin fossiliferous transgressive marine sand, followed by an offlap sequence which commences with marine shale and continues with laminated fluvio marine sediments followed by barriers and/or fluviatile sediments ended by another transgression cycle (Alao *et al.,* 2013; Ejedawe 1981; Weber and Daukoru 1975). The Benin Formation consists of high sand percentage (70–100%) and forms the top layer of the Niger Delta depositional sequence (Alao *et al*., 2013). The massive sands were deposited in continental environment comprising the fluvial realms (braided and meandering systems) of the upper delta plain (Akpabio *et al.,* 2014; Alao *et al.,* 2013; Agbasi 2013). Petroleum occurs within the Agbada Formation of the Niger Delta basin however, several directional trends form an "oil-rich belt" having the largest field and lowest gas:oil ratio (Tamuko 2008; Michele *et al.,* 1999; Akpoyovbike 1978; Ejedawe, 1981; Evamy *et al.,* 1978; Doust and Omatsola, 1990). Hydrocarbon occurrence was originally ascribed to timing of trap formation relative to petroleum migration (earlier landward structures trapped earlier migrating oil) (Tamuko 2008; Michele *et al.,* 1999).

MATERIALS AND METHODS

Materials

In this study, a suite of data which contains GR, density log, sonic log acquired in a well (control well) in Eti-field and post stack seismic volume passing through the well location was provided. The field contains seven (7) wells named as ETI-001 to ETI-007 on the base map (Figure 1b), with ETI-006 (well W-06) acting as the refrence well.

Reservoir delineation, Checkshot correction and Well-to-seismic correlation

The model-based post stack seismic inversion technique was carried out in this study using the full stack seismic data and their associated wavelets as input. Three reservoirs defined as ETI R-1000, ETI R-2000 and ETI R-3000 (Figure 2) were defined from well ETI-006 (reference well). A zero phase ricker wavelet of length 100 ms and 70 Hz frequency was extracted from the full stacked seismic as input (Figure 3). The horizons were mapped with Interpolated picks at the top of reservoir R-ETI 1000 Top (Figure 4). The mapped horizons and control well was used as inputs for the inversion process. The higher the number of available wells and horizons, the better the initial model.

The next step in the inversion procedure was checkshot correction of the p-wave sonic log to match the two-way-time of seismic data. After this, the well data (ETI-006) was tied to the seismic data to procure a correction for the p-wave sonic velocity at the well location. The post stack seismic volume (in SEG-Y format) was loaded through the STRATA sub-program in HRS and ETI-006 well (control well) was placed on the post stack seismic volume. The inversion was done by generating a ricker wavelet from seismic data and convolving it with density and sonic logs from ETI-006 well to produce the synthetic seismogram.

In an effort to improve the match between the synthetic and composite trace at the well location, the synthetic seismogram was correlated to the composite trace (average seismic traces around the well location). The correlation was done across the traces by clicking on the stretch option on HRS interface on the eLOG program; the maximum coefficient of correlation obtained was 0.714 (≈ 71%) at time shift 29 ms down (Figure 5).

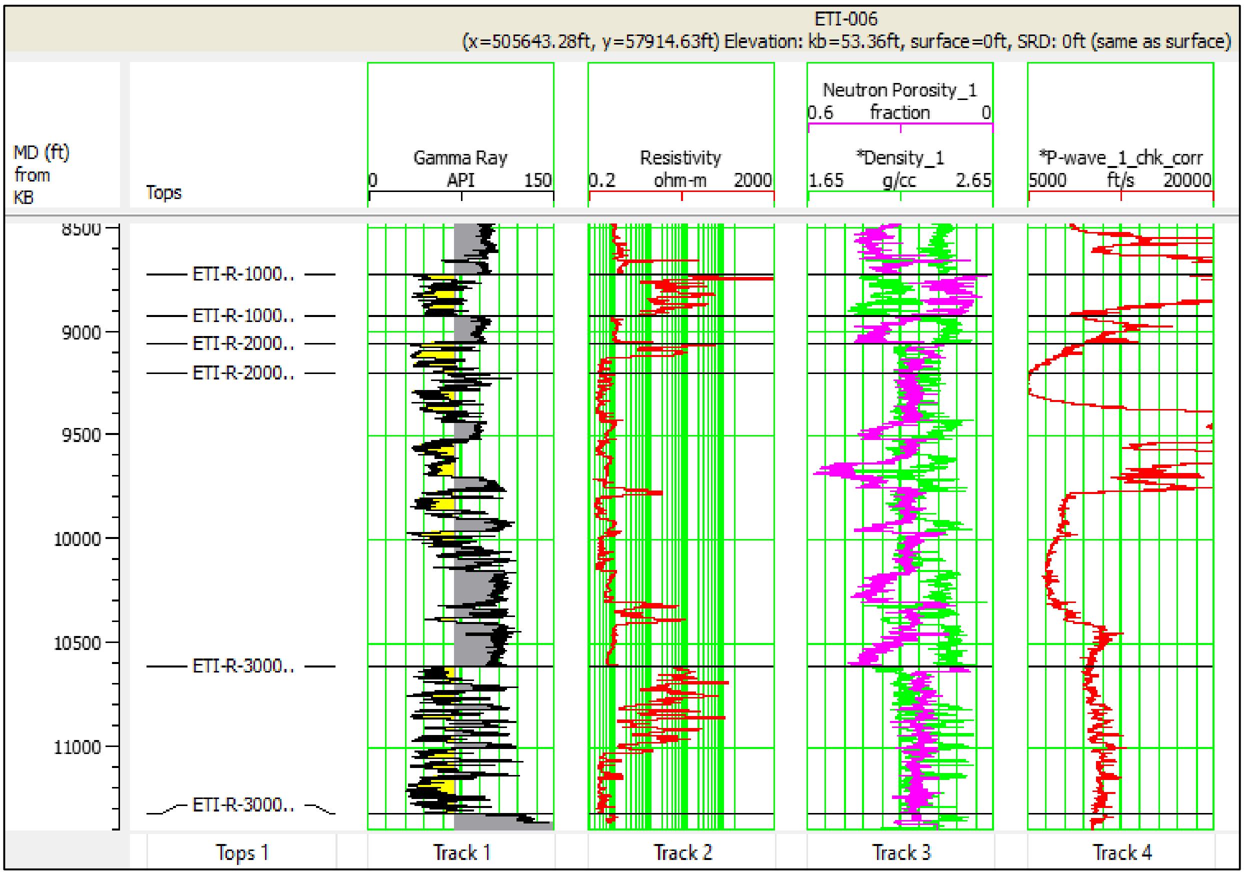

Figure 2: Correlation section across ETI-006 Well showing the Identified Lithology and Reservoir beds.

Print ISSN: 2055-0111 (Print)
Online ISSN: 2055-012X (Online)
Website: https://www.eajournals.org/
Publication of the European Centre for Research Training and Development -UK

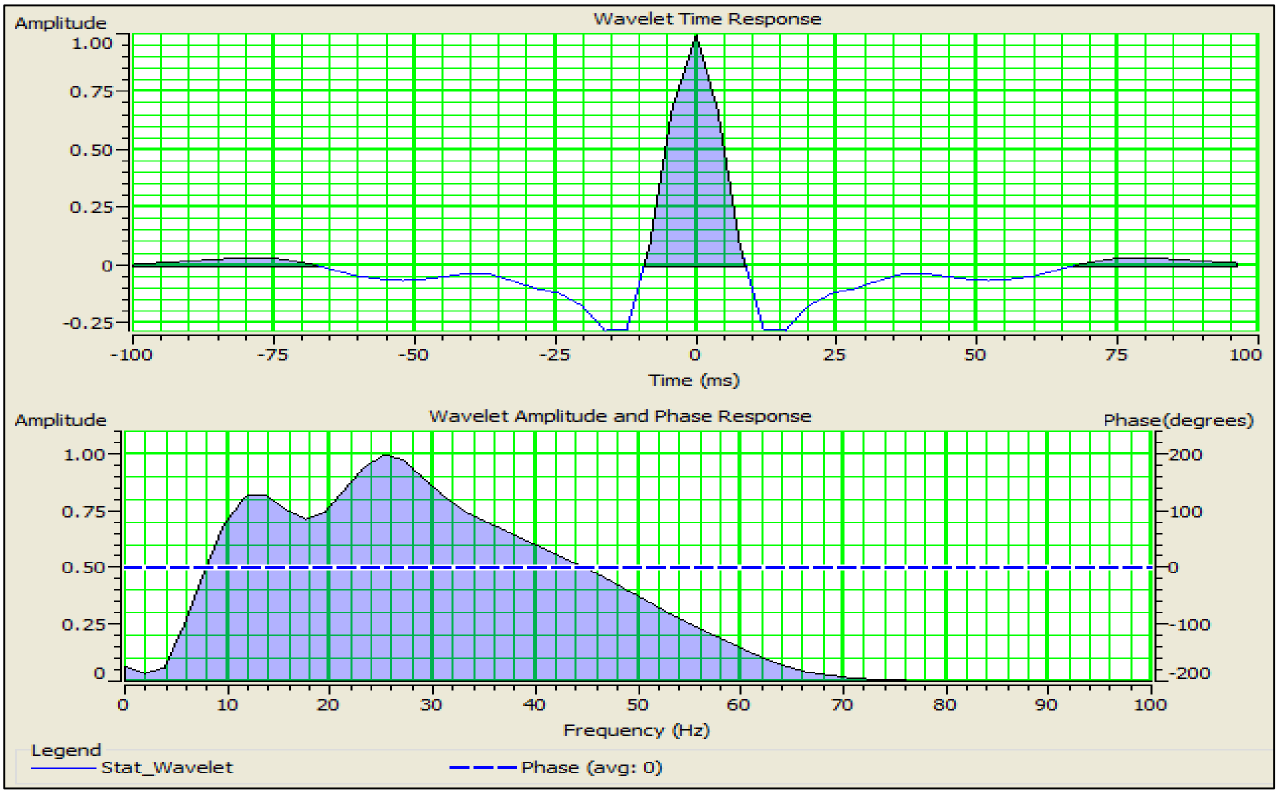

Figure 3: Extracted Seismic Wavelet in time domain and frequency domains with zero phase.

The amplitude spectrum shows the approximate value of the dominant frequency (about 28Hz).

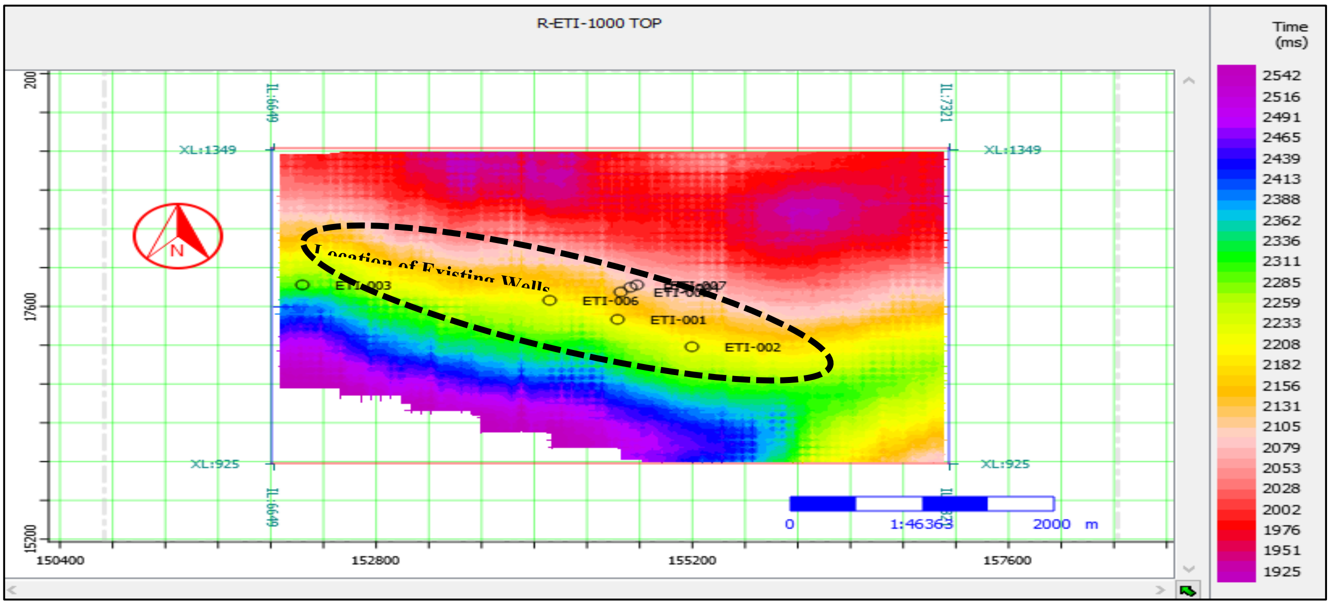

Figure 4: Horizon mapping with Interpolated Picks. Showing reservoir R-ETI 1000 Top and location of the wells.

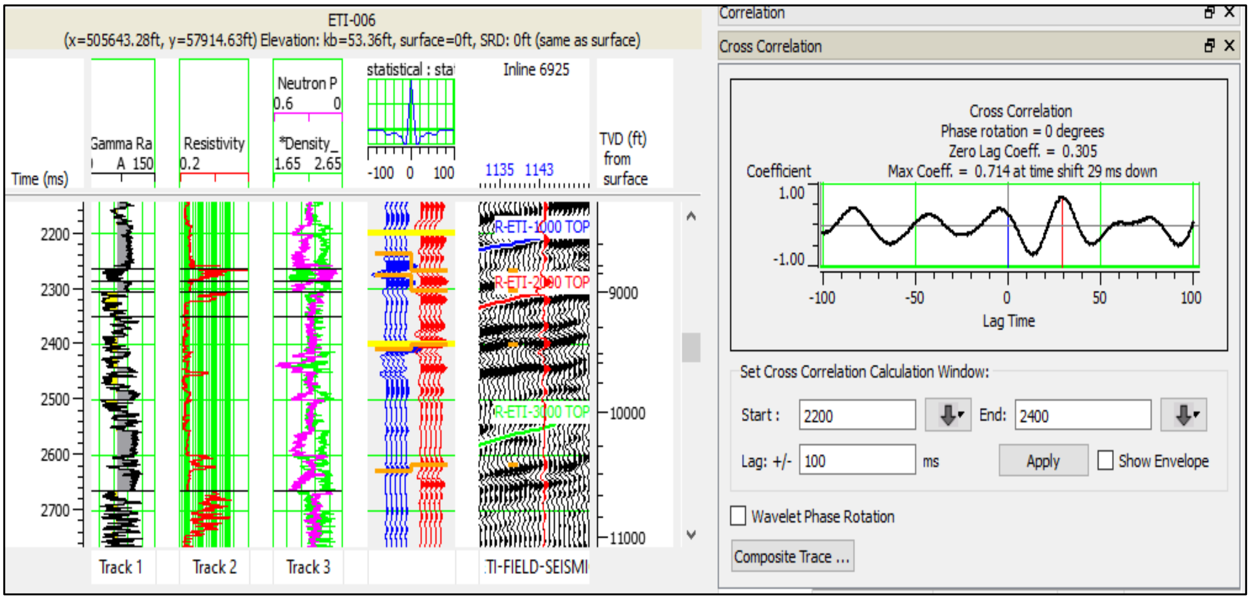

Figure 5: Seismic to well tie analysis and correlation panel with a maximum correlation-coefficient of 0.714 (71.4 %) at time shift of 29ms down.

Initial P-Impedance Model, Model Analysis and Inversion

The initial P-impedance model was created based on the density and P-wave velocity values calculated at log resolution from the control well (ETI-006 well). The initial models for density and P-wave velocity was used as one of the inputs for the inversion analysis process. The result (p-impedance log) were then combined into the post-stack volumes and extrapolated throughout the survey domain (Jason et al., 2008). Seismic data do not contain low frequencies (they are band-limited). Low frequency information is critical in quantitatively inverting acoustic impedance dataset and other reservoir properties sensitive to changes in lithofacies. This prevents the inverted impedance dataset from having the necessary impedance structure required to fit the behaviour of real rocks in the subsurface which is key to making good geological interpretation thus making lithofacies/reservoir prediction difficult based on seismic inversion. To compensate for this, well logs from ETI-006 well (which contain low to very high frequency data) was used to add the low 132 frequencies missing in the seismic bandwidth and to constrain our inversion. This low frequency model was corroborated with well logs and used as the initial guess model for the conjugate gradient perturbation of the impedance model (Jason et al., 2008). The low frequency model assures the inversion result is consistent with the background geological information. Finally, a model–based inversion solution was carried out on the entire 3D data volume. This process requires that the absolute amplitude of the wavelet

British Journal of Earth Sciences Research, 12 (1),42-60,2024
Print ISSN: 2055-0111 (Print)
Online ISSN: 2055-012X (Online)
Website: https://www.eajournals.org/
Publication of the European Centre for Research Training and Development -UK

must be known, and this was resolved by convolving the unscaled wavelet W with the reflectivity of the initial guess model (r) at well (ETI-006 well) and correlated with WT to give WTWr (HRS Strata theory, 1999) to produce an inverted density and P-wave (Zp) acoustic impedance volume which was interpreted. The calculated P-impedance logs were filtered with a 10/15 Hz low-pass filter to retain only the low frequencies not present in the seismic data; and were correlated to check for their consistency, validity of the inversion procedure and the error limits. The low frequency information provided the background trend information for the inversion; in order to make a good geological interpretation. A time slice of inverted P-impedance was extracted from the impedance volume at the top of the reservoir between inlines 6649 and 7321 and crosslines 925 and 1349; to show the lateral variation of acoustic impedance at the well locations.

RESULTS AND DISCUSSION

Figure 6a is the initial model of density at Inline 6649 while initial model of P-Impedance log at Inline 6653 in the vicinity of the control well (ETI-006) is shown in Figure 6b. The colour variation in the initial density and P-impedance models show amplitudes that correspond to density ranging from 1.9603 to 2.4810 g/cc; P-impedance, ranging from 7000 to about 50000 ft/s*g/cc and having a general increase with depth trend.

Figure 7 shows the P-impedance inversion analysis at well ETI-006 location. The initial P-impedance model log (black); original P-impedance log (blue) and inverted P-impedance log (red) is shown. The synthetic (red) and seismic trace (black) correlated well at the well location, giving a near perfect correlation of 0.993686 (correlation coefficient of ≈ 99.4 %). The estimated error was 5533.1 which corresponds to (0.112308) about 11.23 %.

Figure 8 shows the P-impedance inversion result at inline 6655. The result shows large lateral and vertical variations in P-impedance along the seismic profile at this inline (6655).

Specifically, there is a low-impedance structure at the top of the reservoirs (R-ETI-1000, 2000 and 3000) as indicated which can be clearly mapped laterally away from the well, in comparison to the input seismic data. The observed impedance structure is characterized by a varying thickness of sediments. The P-impedance volume can be analysed to predict lateral variations in Poisson's ratio and lithology. P-impedance (a product of rock density and velocity) reduce(s) as seismic waves encounter gas sands (Dubey and Kharagpur, 2021), and on the basis of this assertion, the inverted attribute could provide litho-fluid information within existing reservoirs, and also aid in defining potential reservoirs away from well control. Figure 9 a, b is the 3D impedance block showing inverted impedance structure across ETI-field. Figure 9a is the 3-D block showing impedance slice at inline 7089 while Figure 9b is the 3-D block showing impedance slice at inline 7032 (as indicated by the red arrows). Figure 10 is the P-impedance slice output at top of reservoir R-1000 centered at 10ms window. The Impedance slice was extracted from the P-impedance volume block in Figure 9 a, b. The behavior of the inverted impedance structure across ETI-field for the top of reservoir R-1000 is shown in Figure 10. The low impedance values were observed predominantly towards the location of wells ETI-001, 002, 004, 005 and 006 (as shown by the dark-blue ellipse); while away from the vicinity of the wells impedance values increased towards ETI-003 well (as indicated by the red ellipse). This observation validates that the prediction of lateral variations in rock attributes (particularly impedance in this case) or density and Poisson-ratio which are functions of lithology, at well control and away from well control is possible through the inversion process.

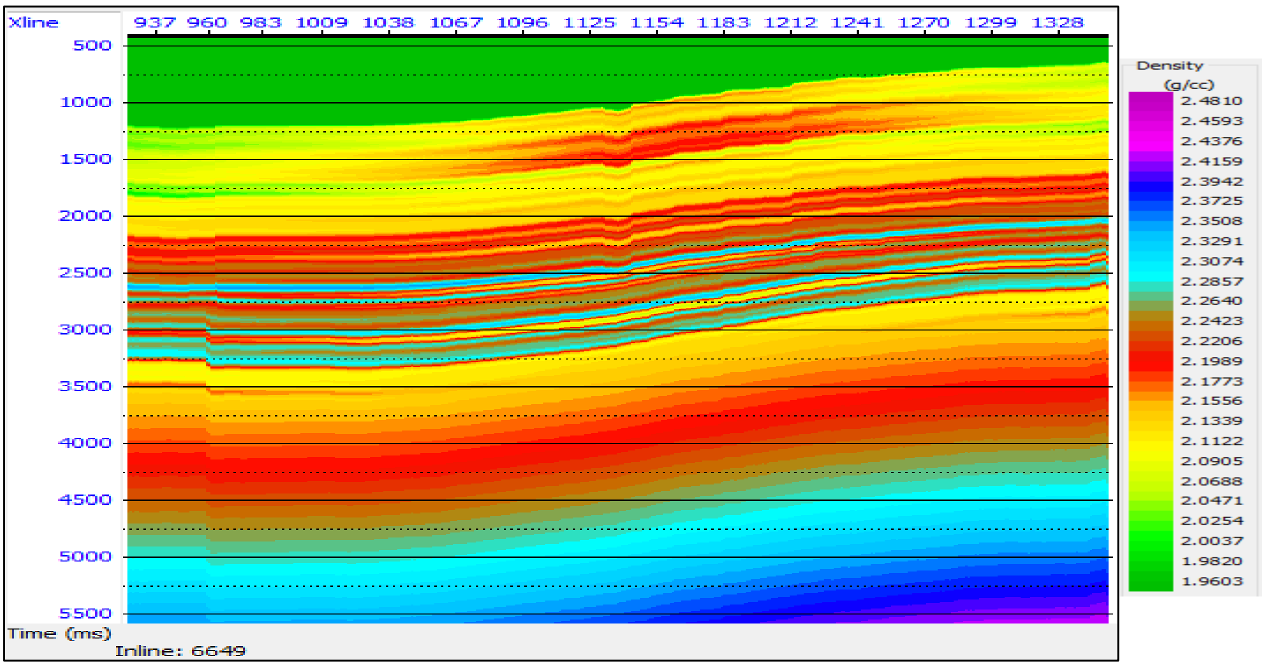

Figure 6 (a): Initial Guess model of density at Inline 6649

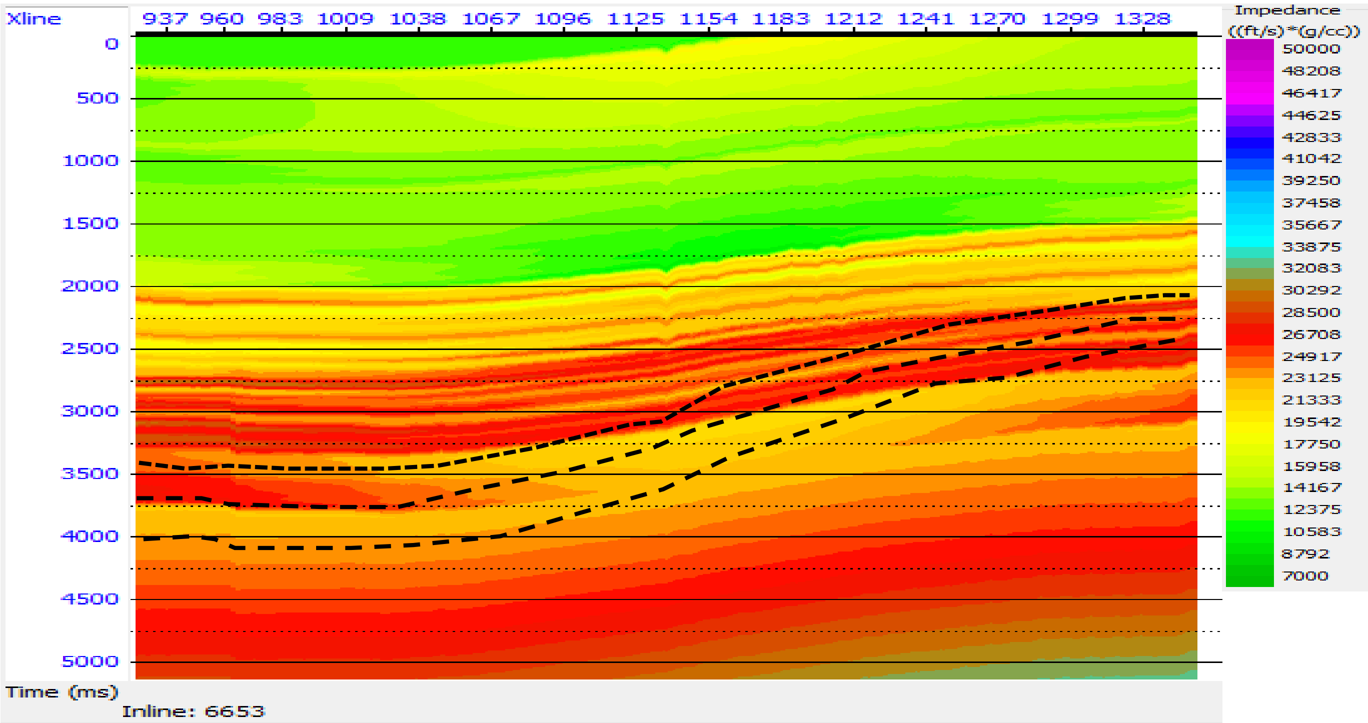

Figure 6 (b): Initial Guess model of Acoustic Impedance at Inline 6653

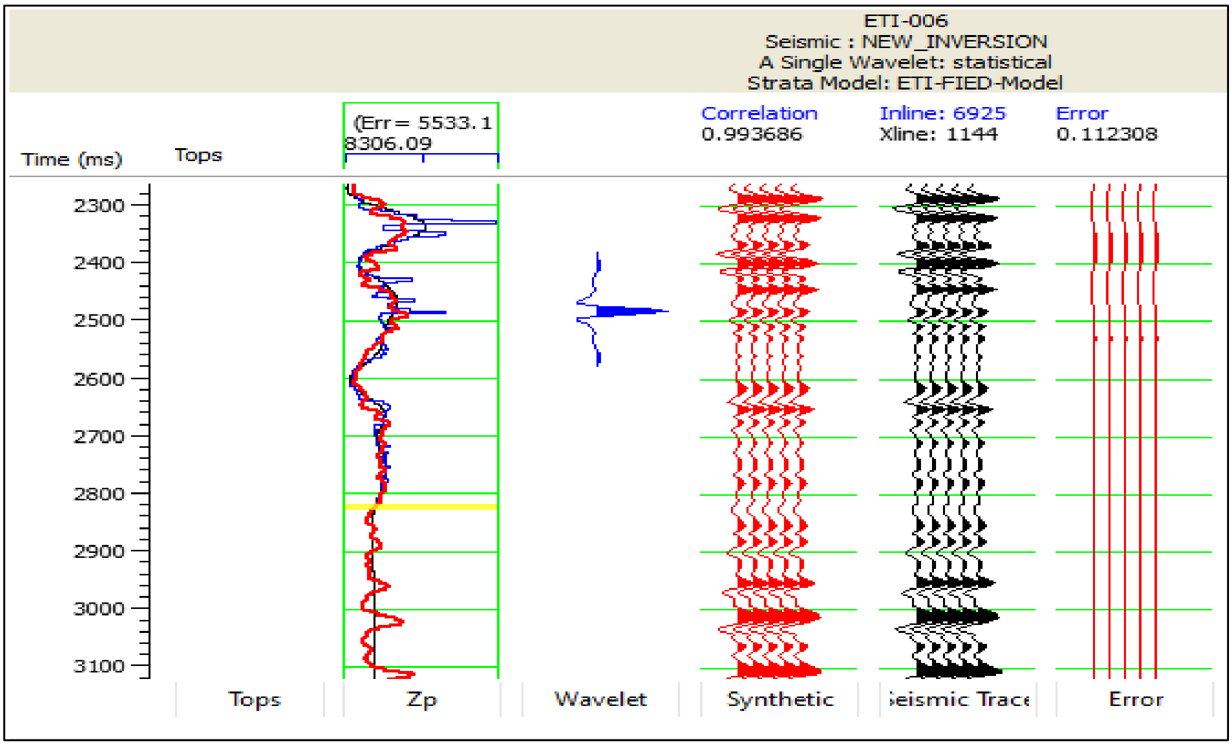

Figure 7: Analysis of P-impedance inversion at well ETI-006: Initial P-impedance model log (black); original P-impedance log (blue); inverted P-impedance log (red).

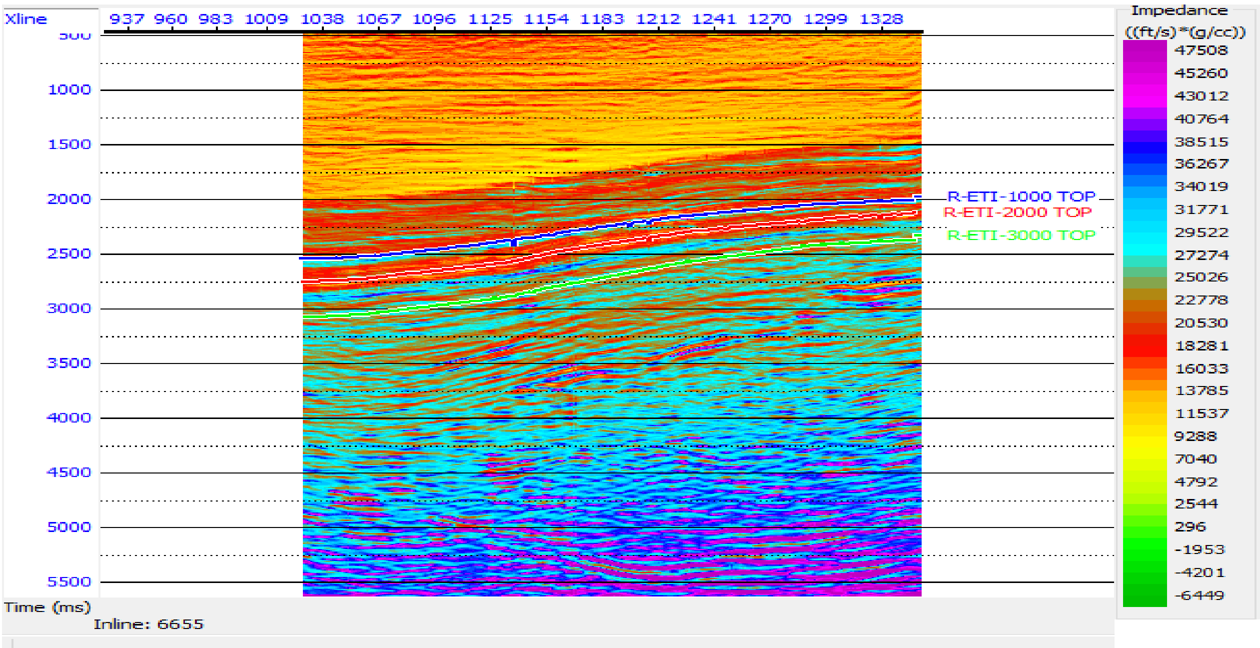

Figure 8: Inversion Analysis with a correlation of 0.99 and error of 0.06. Inverted P-impedance volume of input seismic.

Print ISSN: 2055-0111 (Print)
Online ISSN: 2055-012X (Online)

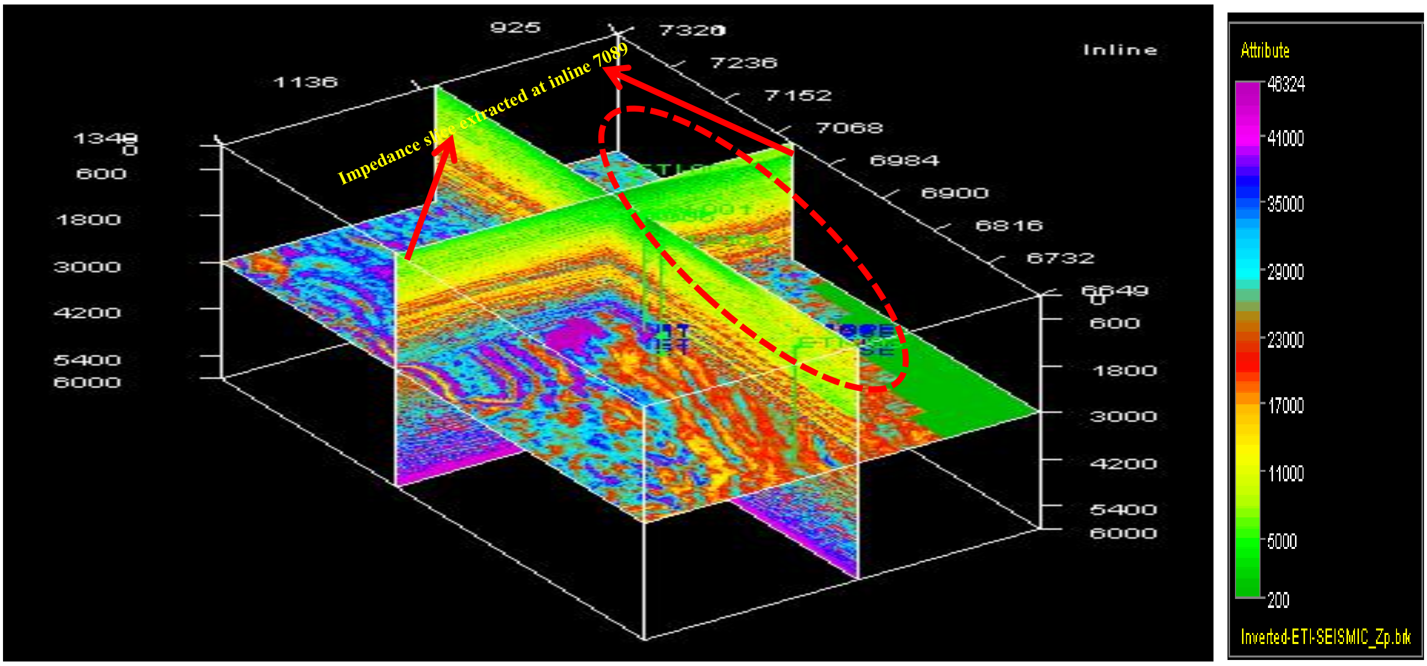

(a)

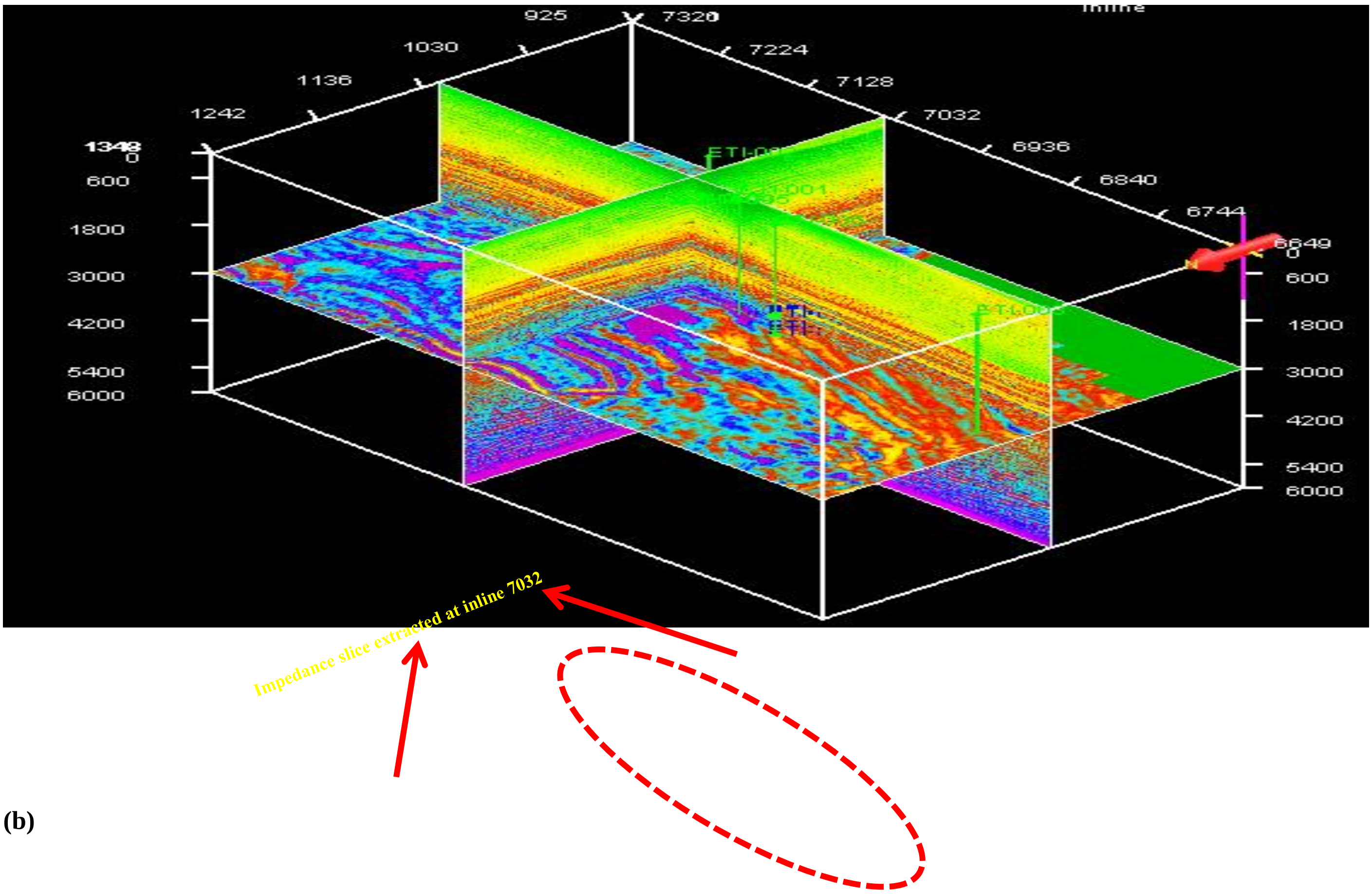

(b)

Figure 9: 3-D impedance block showing inverted impedance structure across ETI-field (a) 3-D block showing impedance slice at inline 7089 (b) 3-D block showing impedance slice at inline 7032.

The inverted attribute could provide litho-fluid and lithofacies information within existing reservoirs and away from the existing reservoirs and this information can be invaluable in delineating more potential reservoir zone often bypassed during drilling thereby enhancing optimum field development which aids in reservoir management decisions. In Figure 10, it was noticed that the impedance variation at top of reservoir R-1000 follows a definite pattern with high impedance values observed predominantly north-west (NW) of the field (red ellipse) while low impedance values were observed predominantly north-east to south-east of the field. Therefore, away from the existing wells more probable prospective reservoir zones have been delineated and can be appraised for production.

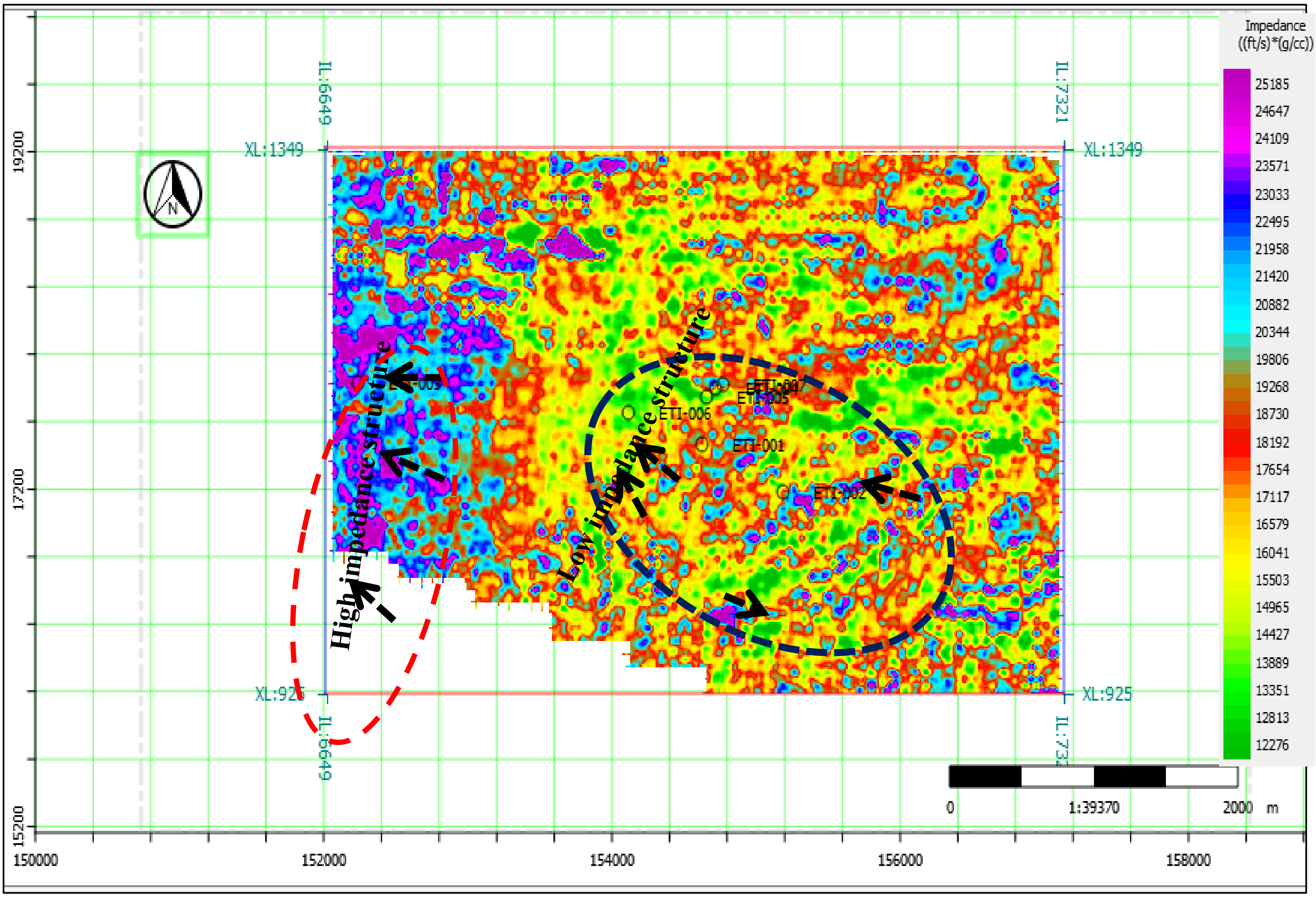

Figure 10: Inversion Analysis. P-Impedance Slice extracted from Impedance volume between Inline 6649-7321 and Xline 925-1349 at top of reservoir R-ETI 1000 window.

CONCLUSION

This study have applied a Model based inversion technique to invert an acoustic impedance structure required to fit the behaviour of rocks in the subsurface using post stack 3D seismic data, for the purpose of lateral prediction of rock properrty and to show lateral and vertical variations in rock property within the reservoir interval. In this study, effort was made to invert post stack 3D seismic data for acoustic impedance in an attempt to characterize lateral variations in rock property in the study field (ETI-field). P-wave velocity and density log data provided the low-frequency input for the inversion to improve data bandwidth, as seismic data is band-limited and does not contain the low frequencies. The results show that acoustic impedance inversion is a veritable tool for delineation of lateral variations in rock properties. The method is capable of revealing distributed zones of low acoustic impedance which can be correlated with prospective reservoir zones away from the wellbore. The process reverses the convolution of the source wavelet and earth's reflectivity in order to obtain the impedance and this has the additional advantage of reducing tuning in the data to improve its reliability. Furthermore, the analysis is able to define the low impedance zones which converge with probable prospective reservoir zones away from control wells. The procedure reverses the convolution of the source wavelet and earth's reflectivity in order to obtain the impedance and this has the additional advantage of reducing tuning in the data to improve its reliability. In general, the results of the seismic inversion procedure in comparison to the input seismic, greatly improved reservoir property interpretability with possible integration with seismic stratigraphy.

Acknowledgements

We wish to express our gratitude to Shell Petroleum Development Company (SPDC) Nigeria for providing the dataset used for this study and to CGG Geosoftware for providing the software used for the study.

REFRENCES

Agbasi, O E (2013). Estimation of water saturation using a modelled equation and Archies equation from wireline logs, Niger Delta Nigeria. *IOSR J. Appl. Phy*. 3 (4): 66-71.

Ahmed H; John C (2016). Distinguishing gas-bearing sandstones reservoirs within mixed Siliciclastic- Carbonate sequence using extended elastic impedance: Nile Delta, Egypt. *Interp*. 4 (4): 435-449.

Alao, PA; Ata, AI; Nwoke, CE; Chuo, YJ; Tzanis, A (2013). Subsurface and Petrophysical studies of Shaly- sand reservoirs targets in Apete field, Niger Delta, *Hind. Geophy*. 10: 1155.

Akpoyovbike AA (1978). Tertiary lithostratigraphy of Niger Delta, *AAPG Bulletin*. 62 (2): 295-300

Akpabio I; Jothson CI; Okechukwu EA; Odunaya TO (2014). Petrophysical characterization of eight wells from wireline log, Niger Delta, Nigeria. *Asian. J. Appl. Sci.* 2 (1): 105

Auster, RC; Borchers, B; Thurber, CH (2005). Parameter estimation and inverse problems. *Elsevier Academic Press.*

Cooke, D; Schneider, W (1983). Generalized inversion of reflection seismic data. *Geophy*. 48(6): 665-676

Doust, H; Omatsola, E (1990). Niger Delta, in Edwards, JD; Santogrossi, PA eds; Divergent/passive Margin basins; *AAPG Memoir* 45: 239–248

Dubey, A.K., Kharagpur, I.I.T. (2012). Reservoir characterization using AVO and seismic inversion techniques, 9th Biennial International Conference & Exhibition on Petroleum Geophysics, Hyderabad.

Duffaut, K; Alsos, T; Landro, M; Rogno, H; and Al-Najjar, N (2000). Shear wave elastic impedance, *The Leading Edge (TLE)*. 1222-1229.

Ejedawe, JE (1981). Patterns of incidence of oil reserves in Niger Delta Basin. *AAPG Bulle.* 65: 1574-1585.\

Evamy, BD; Haremboure, J; Kammerling, R; Knaap, WA; Molloy, FA; Rowlands, PH (1978). Hydrocarbon habitat of tertiary Niger Delta. *AAPG Bulletin.* 62(1): 1 - 39.

Eze, S; Orji, OM; Nnorom, SL; Ubogun, K (2019). Model Based Inversion of Acoustic impedance from Seismic trace for Lithofacies Differentiation: An Application in XY Field Offshore Niger Delta; *Published in J. of Appl. Sci. Environ. Manage. (JASEM); Vol.23(9). DOI: https://dx.doi.org/10.4314/jasem.v23i9.12; P. 1677-1684.*

Hamson-Russell Ltd (1999). The theory of Strata program

Jason, M; Crank, MC; Don, L (2008). Acoustic impedance inversion and Co_2 flood detection at the Alder flats ECBM Project. *CREWES Research Report*. 20

Karbalaali, H; Shadizadeh, SR; Ali, R (2013). Delineating hydrocarbon bearing zones using Elastic Impedance Inversion; A persian Gulf example. *Iranian. J. Oil and Gas science and technology*. 2 (2): 8-19

Lavergne, M; William, C (1977). Inversion of seismograms and pseudo-velocity logs. *Geophys. Prosp.* 25: 232-250

Lindseth, RO (1979). Synthetic sonic logs-a process for stratigraphic interpretation. *Geophysics.* 44(1): 3-26

Michele, LWT; Ronald, RC; Michael, EB (1999). The Niger Delta Petroleum system; Niger Delta province, Nigeria, Cameroon and Equitorial Guinea. *Africa Open file report*: 50-51

Nadin, PA; Kusznir, NJ (1995). Palaeocene uplift and Eocene subsidence in the Northern North Sea Basin from 2D forward and reverse stratigraphic modelling. *J. of the Geolo. Society*. 152 (5): 833-848

Ogagarue, DO; Alaminiokuma, GI (2016). Lateral Rock Property Prediction by Post Stack Acoustic Impedance Inversion: A case study from offshore Niger Delta. *Int. J. of Sci. Basic and Appl. Research (IJSBAR).* 26(3): 1-13

Ogagarue, DO (2016). A comparative study of Acoustic and Elastic Impedance Seismic Models for Rock Property Prediction: An example from XYZ Field, Nigeria. *Int. J. of Sci. Basic and Appl. Research (IJSBAR).* 26(3): 24-34

Orife, JM; Avbovbo, AA (1982). Stratigraphic and Unconformity traps in the Niger Delta

Okoli, EA; Onyekuru, SI; Agbasi, OE; Zaidoon, TA (2018). Application of Model-based inversion technique in a field in the coastal swamp depobels, Niger Delta. *Int. J. Adv. Geosciences*. 6 (1): 122-126

Parvaneh, K (2015). Structure-constrained relative acoustic Impedance using Stratigraphic Co-ordinates. *Geophysics.* 80 (3): 63-67

Sheriff, RE (2002). Encyclopedic Dictionary of Applied Geophysics. *Society of Exploration Geophysics, Tulsa, Oklahoma, USA*, 13 editions

Short, KC; Stauble, AJ (1967). Outline of geology of Niger Delta. *AAPG Bulletin*. 51(5): 761 – 779

Tamuko, OJ (2008). 3D Seismic structural interpretation and Petrophysical Evaluation of X-field, Niger Delta Basin, Nigeria, B.Tech Unpublished Project, *Federal University of Technology Akure (FUTA)*

Weber, KJ; Daukoru, EM (1975). Petroleum Geology of the Niger Delta. *Proceedings of the 9th World Petroleum Congress Tokyo. Appl. Sci. publishers, Ltd, London.* 2: 202-221

Yi Zhang; Jiangwo, Y; Fei Li; Chao, C; Bao, M; Shuanggen, J; James HD (2015). A new bound constraints method for 3D Potential field data Inversion using Lagrangian Multipliers. *Geophys. J. Int.* 2(1): 267-275.